Synthesis, Crystal Growth and Structure Investigations of Rare-Earth Disilicates and Rare-Earth Oxyapatites

A. Nørlund Christensen,*,a R. G. Hazella and A. W. Hewatb

aDepartment of Inorganic Chemistry, Aarhus University, DK-8000 Aarhus C, Denmark and bMax von Laue–Paul Langevin Institute, PO Box 156, F-38042 Grenoble 9, France

Christensen, A. N., Hazell, R. G. and Hewat, A. W., 1997. Synthesis, Crystal Growth and Structure Investigations of Rare-Earth Disilicates and Rare-Earth Oxyapatites. – Acta Chem. Scand. 51: 37–43. © Acta Chemica Scandinavica 1997.

The rare-earth disilicates $RE_2Si_2O_7$ ($RE = La$, Nd, Sm, Eu, Gd, Tb, Dy, Ho, Er and Y) and the rare-earth oxyapatites $RE_{9.33} \square_{0.67}(SiO_4)_6O_2$ ($RE = La$, Nd and Eu) were synthesized in solid-state reactions at temperatures from 1050 to 1500 °C. Single crystals of the disilicates $Ho_2Si_2O_7$, $Er_2Si_2O_7$ and $Y_2Si_2O_7$ and of the oxyapatites $Eu_{9.33} \square_{0.67}(SiO_4)_6O_2$ and $Dy_{9.33} \square_{0.67}(SiO_4)_6O_2$ were grown in a flux growth mode in the temperature interval 1260–960 °C from a flux containing Bi_2O_3 and V_2O_5. Purity of single crystals and reaction products was investigated by X-ray single-crystal and powder-diffraction techniques.

X-Ray single-crystal diffraction analyses are reported on $Ho_2Si_2O_7$ and $EuVO_4$. $Ho_2Si_2O_7$ type D is monoclinic $P2_1/c$ with $Z=4$ and $a=4.6868(5)$, $b=10.8618(12)$, $c=5.5872(5)$ Å, $\beta=95.993(7)°$. $EuVO_4$ is tetragonal $I4_1/amd$ with $Z=4$ and $a=7.2480(9)$, $c=6.3778(10)$ Å.

Neutron powder diffracton analyses are reported on $Er_2Si_2O_7$, $Ho_2Si_2O_7$ and $Y_2Si_2O_7$ all of type D structure and on the oxyapatites $La_{9.33} \square_{0.67}(SiO_4)_6O_2$ and $Nd_{9.33} \square_{0.67}(SiO_4)_6O_2$. The type D structure is monoclinic with $P2_1/c$ and $Z=4$. $Er_2Si_2O_7$ has $a=4.6943(4)$, $b=10.8097(10)$, $c=5.5646(4)$ Å, $\beta=96.037(4)°$. $Ho_2Si_2O_7$ has $a=4.6929(5)$, $b=10.8627(12)$, $c=5.5895(5)$ Å, $\beta=96.017(4)°$. $Y_2Si_2O_7$ has $a=4.6916(4)$, $b=10.8521(10)$, $c=5.5872(5)$ Å, $b=96.040(3)°$. The rare-earth oxyapatite structure is hexagonal with $P6_3/m$ and $Z=1$. $La_{9.33} \square_{0.67}(SiO_4)_6O_2$ has $a=9.7259(10)$ and $c=7.1899(3)$ Å, and $Nd_{9.33} \square_{0.67}(SiO_4)_6O_2$ has $a=9.5731(8)$ and $c=7.0336(2)$ Å.

The synthesis of high-temperature phases of the rare-earth disilicates $RE_2Si_2O_7$ ($RE = La$, Ce, Pr, Nd, Sm, Gd, Tb, Dy, Ho, Er, Tm, Yb, Lu and Y) from the melt, using a crucible-free technique, was reported recently.[1] The technique used was to melt the end of a ceramic rod of $RE_2Si_2O_7$ and to collect the droplets of the compound on a tray of BN, on which they froze to the silicate. However, some of the samples made in this way contained rather large quantities of impurity phases which were, as examples, $Ho_{9.33} \square_{0.67}(SiO_4)_6O_2$ in the $Ho_2Si_2O_7$ sample and $Y_{9.33} \square_{0.67}(SiO_4)_6O_2$ in the sample of $Y_2Si_2O_7$.[1] The traditional way of synthesis for the rare-earth disilicates is to apply solid-state sintering reaction in which pellets of the oxide mixtures are kept at temperatures in the range 1200–1600 °C for time periods up to 100 h. These heat treatments are repeated a number of times for each sample after grinding and formation of new pellets after each treatment to insure homogeneity. This synthesis technique was applied in the present work.

Four high-temperature forms of $RE_2Si_2O_7$ have been reported.[2] The structure type G is monoclinic for $RE =$

La to Sm, type F is triclinic for $RE = Sm$ and Eu, type E is orthorhombic for $RE = Eu$ to Ho, and type D is monoclinic for $RE = Ho$ and Er and exists also for Y. In addition, type C is monoclinic for $RE = Ho$ to Lu and is most likely stable at high as well as at low temperatures for $RE = Tm$ to Lu. The geometry in the $Si_2O_7^{6-}$ ions in the different structure types is so that the Si–O–Si angle is 180° in the type C and D structures, determined by the symmetry of the space groups of the two structure types. The Si–O–Si angle in the type G structures cluster around 132°, and are in the type E structures found in the interval 150–160°.[1] The type F structure is not known in detail.

In the type E structures of $Ho_2Si_2O_7$ and $Y_2Si_2O_7$ it was found from profile analysis of neutron diffraction powder patterns that the Si–μ–O distances (μ–O denotes the bridge oxygen atom) were longer than reported earlier for the type E structure of $Y_2Si_2O_7^3$ and $Gd_2Si_2O_7$.[4] To clarify this ambiguity a detailed structure analysis of the type E structures of $RE_2Si_2O_7$ ($RE = Gd$, Tb, Dy, Ho, and Y) is planned. Single crystals of $RE_2Si_2O_7$ ($RE = Ho$, Er, and Tm for type C, $RE = Ho$ and Er for type D, and $RE = Dy$ for type E structure) have been obtained

* To whom correspondence should be addressed.

in a flux growth method.[5] The single crystals were obtained by slow cooling of melts containing Bi_2O_3 and V_2O_5. Crystal growth by a flux method has been made for the compounds $Ho_2Si_2O_7$ (type *D*) $Er_2Si_2O_7$ (type *C*), $Y_2Si_2O_7$ (type *D*), $Eu_{9.33}\square_{0.67}(SiO_4)_6O_2$, and $Dy_{9.33}\square_{0.67}(SiO_4)_6O_2$ to obtain samples for single-crystal structure analysis and the results of the growth experiments are reported below.

Experimental

Solid-state synthesis and crystal growth. The following chemicals were used in the synthesis: SiO_2, kieselgur, V_2O_5 (Merck), La_2O_3 (Johnson Matthey), Ho_2O_3, Er_2O_3, Bi_2O_3 (Fluka), Sm_2O_3, Eu_2O_3, Ho_2O_3, Y_2O_3 (Auer Remy), and Nd_2O_3, Eu_2O_3, Gd_2O_3, Tb_4O_7, Dy_2O_3, Ho_2O_3, Er_2O_3 (Rhone-Poulenc). Stoichiometric mixtures of the rare-earth oxides and kieselgur were pressed into 10 or 25 mm diameter pellets in moulds of cemented carbides and heated twice or up to five times in an electric furnace with intermediate grindings and pressing into new tablets in the solid-state sintering reactions. The experimental conditions listing temperature and time for the first and last heat treatment are listed in Table 1. The tablets were placed in Al_2O_3 crucibles or on blocks of Al_2O_3. In some cases, minor reactions between the pellets and the Al_2O_3 support were observed. The mass of the reaction mixture was typically about 20 g for each charge. To obtain a sample of the type *F* structure of $Sm_2Si_2O_7$ a 10 mm diameter sample of the compound was heated in an RF heating coil with a graphite susceptor in a He atmosphere.[6] The sintering temperature for this experiment could not be recorded.

The experimental conditions for the flux growth experiments are listed in Table 2. The melt was kept in a 50 ml platinum crucible placed in a 150 ml Al_2O_3 crucible on a support of granulated ZrO_2. The growth furnace used has been described previously.[7] Crystal growth by a self-nucleation was achieved by a slow cooling from the maximum to minimum temperature listed in Table 2. From the latter temperature the furnace was cooled fast to room temperature. To remove the V_2O_5–Bi_2O_3 flux from the grown crystals the platinum crucible was placed upside down on a porous support of magnesium oxide in a platinum bowl and heated to the minimum temperature (see above) in a furnace for 5 h. By this treatment, the flux was sucked into the magnesium oxide support and the grown single crystals could easily be removed from the platinum crucible.

X-Ray diffraction. X-Ray powder patterns were recorded at 25 °C of the samples from the solid-state synthesis and from the crystal growth experiments on a Stoe–Stadi powder diffractometer with a position-sensitive detector. The diffractometer was calibrated with a silicon standard ($a = 5.430\,50$ Å) and Cu $K_{\alpha1}$ radiation was used ($\lambda = 1.540\,598$ Å). The phases identified from the powder patterns are listed in Tables 1 and 2.

Three-dimensional single-crystal X-ray diffraction data were measured on a Huber four-circle diffractometer on a crystal of $Ho_2Si_2O_7$ type *D* and on a crystal of $EuVO_4$, and experimental conditions and crystallographic data for these two structures are displayed in Table 3.

Neutron powder diffraction. The neutron diffraction powder patterns were measured of the rare-earth silicates at 27 °C on the powder diffractometer D1A at Institut Laue-Langevin, Grenoble. Experimental conditions for the measurements and unit cells and space groups for the five compounds are listed in Table 4.

Results and discussion

The purpose of the solid-state synthesis was to produce samples of $RE_{9.33}\square_{0.67}(SiO_4)_6O_2$ and $RE_2Si_2O_7$ for further structure investigations by neutron powder diffraction technique. In the cases of $Eu_2Si_2O_7$ and $Sm_2Si_2O_7$ the goal was to produce samples of the structure type *F* for detailed structure analysis using X-ray powder diffraction data. The purpose of the crystal growth synthesis was to test the possibility of growing single crystals of the high-temperature phases from a flux. Of special interest was the possible growth of single crystals of $Eu_2Si_2O_7$ type *F*.

Oxide mixtures with a stoichiometric composition to produce the apatite forms $RE_{9.33}\square_{0.67}(SiO_4)_6O_2$ formed readily these compounds at 1400 °C (Table 1). This was also the case for oxide mixtures with a composition to produce $RE_2Si_2O_7$ (Table 1) except in the cases of Sm and Eu, for which a strong tendency to produce the apatite forms was observed in a number of the experiments. This may be related to the position of Sm and Eu in the row of lanthanides where at least Eu^{2+} ions may be formed in reduction of Eu^{3+}, or to the fact that the two rare-earth oxides reacted with the Al_2O_3 crucibles.

In the binary system Ho_2O_3–SiO_2 a phase with the composition $Ho_2Si_6O_{15}$ has been reported,[8] but a structure of a holmium silicate with this composition has not been reported. Attempts were made to synthesize the holmium silicate reported to have the composition $Ho_2Si_6O_{15}(Ho_2O_3 \cdot 6SiO_2)$.[8] As Y^{3+} has approximately the same ionic radius as Ho^{3+}, attempts were also made to make an yttrium silicate with the composition $Y_2Si_6O_{15}$. Pellets of the two oxides and SiO_2 (kiselgur) with the nominal composition $Ho_2O_3 \cdot 6SiO_2$ and $Y_2O_3 \cdot 6SiO_2$ and a pellet of SiO_2 (kiselgur) were placed in a boat of Al_2O_3 and kept in a furnace at 1100 °C for 68 days (Table 1). X-Ray powder patterns of the SiO_2 pellets showed that it was cristobalite, those of the $Y_2O_3 \cdot 6SiO_2$ pellet showed that it was a mixture of $Y_2Si_2O_7$ type *C* and cristobalite, and those of the $Ho_2O_3 \cdot 6SiO_2$ pellet showed that it was a mixture of $Ho_2Si_2O_7$ type *B* and cristobalite. The X-ray powder pattern listed in Ref. 8, Table 5, for the compound $Ho_2O_3 \cdot 6SiO_2$ is indeed very similar to that of $Ho_2Si_2O_7$

Table 1. Experimental conditions for the solid-state synthesis of polycrystalline samples of rare-earth silicates.

Stoichiometric mixtures to produce $RE_{9.33}\square_{0.67}(SiO_4)_6O_2$

Quantities/g	RE_2O_3	SiO_2	First heat treatment/°C	Last heat treatment/°C	Reaction time/h	Product	Structure type	Impurity phase
La_2O_3	20.63	4.89	1400	1400	125	$La_{9.33}\square_{0.67}(SiO_4)_6O_2$	Apatite	None
Nd_2O_3	4.89	1.12	1400	1400	200	$Nd_{9.33}\square_{0.67}(SiO_4)_6O_2$	Apatite	None
Eu_2O_3	4.93	1.08	1300	1400	100	$Eu_{9.33}\square_{0.67}(SiO_4)_6O_2$	Apatite	None

Stoichiometric mixtures to produce $RE_2Si_6O_{15}$

Quantities/g	RE_2O_3	SiO_2	Heat treatment/°C	Reaction time/d	Product	Structure type	Impurity phase
Ho_2O_3	5.67	5.41	1100	68	$Ho_2Si_2O_7$	B	Cristobalite
Y_2O_3	4.52	7.21	1100	68	$Y_2Si_2O_7$	C	Cristobalite
		5.50	1100	68	Cristobalite		

Stoichiometric mixtures to produce $RE_2Si_2O_7$

Quantites/g	RE_2O_3	SiO_2	First heat treatment/°C	Last heat treatment/°C	Reaction time/h	Product	Structure type	Impurity phase
La_2O_3	27.54	10.78	1350	1400	150	$La_2Si_2O_7$	G	None
Nd_2O_3	15.52	5.54	1300	1400	125	$Nd_2Si_2O_7$	A	None
Eu_2O_3	19.84	6.78	1350	1400	200	$Eu_2Si_2O_7$	E	None
Eu_2O_3	9.15	3.12	1400	1050	150	$Eu_{9.33}\square_{0.67}(SiO_4)_6O_2$	Apatite	None
Eu_2O_3	9.15	3.12	1300	1050	150	$Eu_{9.33}\square_{0.67}(SiO_4)_6O_2$	Apatite	None
Sm_2O_3	5.67	1.96	1300	1400	250	$Sm_2Si_2O_7$	A^c	None
Sm_2O_3	20.14	6.94	1350	1400	200	$Sm_2Si_2O_7$	A	None
Sm_2O_3	17.51	6.03	1300					
Gd_2O_3	5.17	1.76	1300	1400	150	$Gd_2Si_2O_7$	E	None
Tb_4O_7	25.26	8.12	1300	1400^a	150	$Tb_2Si_2O_7$	E	None
Dy_2O_3	15.01	4.83	1300	1400	150	$Dy_2Si_2O_7$	B	None
Dy_2O_3	25.25	8.14	1300	1400^a	150	$Dy_2Si_2O_7$	E	None
Ho_2O_3	4.19	2.00^b	1400	1130	100	$Ho_2Si_2O_7$	D	Formation of a glass
Ho_2O_3	11.34	3.61	1450	1450	200	$Ho_2Si_2O_7$	D	None
Er_2O_3	14.02	4.40	1450	1400	225	$Er_2Si_2O_7$	D	None
Y_2O_3	6.77	3.60	1450	1450	200	$Y_2Si_2O_7$	D	None
Y_2O_3	34.57	18.39	1400	1500	200	$Y_2Si_2O_7$	D	None

^{a} The temperature control failed in these experiments and the actual temperature in the furnace may have been higher than the reported value of 1400 °C. ^{b} To produce a silicate with the composition $Ho_2Si_3O_9$ (reported in Ref. 8). ^{c} Converted to type F when heated in ADL high-frequency furnace.

Table 2. Experimental conditions for the flux growth experiments using the molar ratios: 7.14 RE_2O_3: 21.43 SiO_2: 57.15 Bi_2O_3: 14.28 V_2O_5.

Quantities/g	RE_2O_3	SiO_2	Bi_2O_3	V_2O_5	T_{max}/°C	T_{min}/°C	Cooling rate/ °C h^{-1}	Main product	Structure type	Impurity phase
Eu_2O_3	3.77	1.93	39.94	3.90	1260	960	1.5	$Eu_{9.33}\square_{0.67}(SiO_4)_6O_2$		$EuVO_4$
Dy_2O_3	3.99	1.93	39.94	3.90	1260	960	1.5	$Dy_{9.33}\square_{0.67}(SiO_4)_6O_2$		None
Ho_2O_3	4.05	1.93	39.94	3.90	1260	960	1.5	$Ho_2Si_2O_7$	Type D	None
Er_2O_3	4.10	1.93	39.94	3.90	1260	960	1.5	$Er_2Si_2O_7$	Type C	None
Y_2O_3	2.42	1.93	39.94	3.90	1260	1140	1.5	$Y_2Si_2O_7$	Type D	None

type *B*. Two powder patterns are listed in Ref. 8 for two modifications of a holmium silicate with the composition $Ho_2O_3\cdot3SiO_2$. The pattern listed for the low-temperature modification of this compound (Ref. 8, Table 3) is indeed similar to that of $Ho_2Si_2O_7$, type *C*, and the pattern listed for the high-temperature modification of the compound (Ref. 8, Table 4) is the same as that of $Ho_2Si_2O_7$,

type *D*. The phase diagram reported for the system Ho_2O_3–SiO_2 in Ref. 8 has thus most likely severe errors. Attempts were also made in this investigation to synthesize a holmium silicate with the composition $Ho_2O_3\cdot3SiO_2$. This resulted in formation of samples of $Ho_2Si_2O_7$, type *D*, containing the surplus SiO_2 as cristobalite (Table 1).

Table 3. Experimental data and unit cell parameters for EuVO$_4$ and for Ho$_2$Si$_2$O$_7$, type *D*.

	EuVO$_4$	Ho$_2$Si$_2$O$_7$
a/Å	7.2480(9)	4.6868(5)
b/Å	7.2480(9)	10.8618(12)
c/Å	6.3778(10)	5.5872(5)
α/°	90.0	90.0
β/°	90.0	95.993(7)
γ/°	90.0	90.0
Cell volume/Å^3	335	283
Space group	I4$_1$/amd	P2$_1$/c
Z	4	4
Density (calc)/g cm^{-3}	5.29	5.85
Size of crystal/mm	0.250 × 0.033 × 0.094	0.150 × 0.220 × 0.080
Linear absorption coefficient, μ/cm^{-1}	215	151
Transmission between	0.16–0.56	0.09–0.23
No. of measured reflections (including two standards)	2655	4717
R$_{intern}$ of reflections (%)	4.8	1.9
No. of independent reflections	2544	4250
No. of reflections with I > 3σ(I)	304	1112
Scan method	ω–2θ	ω–2θ
θ$_{max}$/°	36	36
T/K	298	298
Wavelength/Å	0.7107	0.56090

The crystal growth experiments from a Bi$_2$O$_3$–V$_2$O$_5$ flux resulted in formation of single crystals of the high-temperature forms, type *D*, of Ho$_2$Si$_2$O$_7$ and Y$_2$Si$_2$O$_7$, which again illustrates the similarity between the Ho^{3+} and Y^{3+} ions. The type *D* structures were also obtained of the two compounds in the solid-state sintering reactions at 1450 °C (Table 1). However, the rare-earth disilicates were not obtained in the crystal growth experiments of Eu and Dy where the apatite forms Eu$_{9.33}$ □$_{0.67}$(SiO$_4$)$_6$O$_2$ and Dy$_{9.33}$ □$_{0.67}$(SiO$_4$)$_6$O$_2$ were the single crystals obtained. In addition, well formed single crystals of europium vanadate, EuVO$_4$ were formed in the europium silicate crystal growth experi-

ment. It is remarkable that the two apatite compounds are formed instead of the rare-earth disilicates. The composition of the flux may favour the formation of one silicate or modification of a rare-earth silicate to other compounds.[5] However, in the solid-state sintering experiments the tendency of the formation of Eu$_{9.33}$ □$_{0.67}$(SiO$_4$)$_6$O$_2$ was strong, also from stoichiometric mixtures to produce Eu$_2$Si$_2$O$_7$.

Single-crystal X-ray diffraction investigation of the structures of EuVO$_4$ and Ho$_2$Si$_2$O$_7$, type D.

Structure determination of EuVO$_4$. A needle-shaped single crystal of EuVO$_4$ was selected using the polarising microscope, and precession photographs confirmed the space group I4$_1$/amd. The X-ray diffractometer data were collected on a Huber four-circle diffractometer. Unit cell parameters and other experimental data are listed in Table 3.

The structure was solved by direct methods using the SHELX86 program.[9] This gave the position of all the atoms of the structure and a difference Fourier map did not indicate any additional electron density. The model of the structure was refined using the least squares program LINUS,[10] with scattering contributions from neutral atoms,[11] and with correction for anomalous dispersions.[12] The weights used in the refinements were $1/\sigma(I)$ with $\sigma(I) = [\sigma_{count}(F^2) + 1.03F^2]^{1/2} - |F|$ and $\sigma_{count}(F^2)$ is (number of counts)$^{1/2}$. The final R-values were $R_F = 2.1\%$ and $R_w = 3.5\%$. Atomic coordinates and displacement parameters are listed in Table 5 and interatomic distances and bond angles are in Table 6. All the rare-earth vanadates and that of yttrium can have the zircon structure,[13] and the crystal structures of YVO$_4$ and of ErVO$_4$ have been reported.[14,15] The interatomic distances found in the structure of EuVO$_4$ have a higher precision than the distances reported previously for the structures of YVO$_4$ and ErVO$_4$.

Structure determination of Ho$_2$Si$_2$O$_7$ type D. A single crystal of Ho$_2$Si$_2$O$_7$ was selected using the polarising microscope, and precession photographs confirmed the

Table 4. Experimental data and unit-cell parameters for rare-earth silicates measured at the neutron powder diffractometer.

Compound[a]	A	B	C	D	E
Diffractometer	D1A	D1A	D1A	D1A	D1A
2θ$_{min}$/°	10.0	10.0	10.0	10.0	24.1
2θ$_{max}$/°	147.0	147.0	147.0	147.0	147.0
Δ2θ/°	0.05	0.05	0.05	0.05	0.05
λ/Å	1.909	1.909	1.909	1.909	1.909
Max. sin θ/λ/Å^{-1}	0.50	0.50	0.50	0.50	0.50
Diameter of vanadium can/mm	16	12	12	12	12
a/Å	9.726(1)	9.573(1)	4.6943(4)	4.6925(5)	4.6916(4)
b/Å	9.726(1)	9.573(1)	10.8097(10)	10.8627(12)	10.8521(10)
c/Å	7.190(1)	7.034(1)	5.5646(4)	5.5895(5)	5.5872(5)
β/°			96.037(4)	96.017(4)	96.040(3)
Space group	P6$_3$/m	P6$_3$/m	P2$_1$/c	P2$_1$/c	P2$_1$/c

[a] A: La$_{9.33}$ □$_{0.67}$(SiO$_4$)$_2$O$_2$; B: Nd$_{9.33}$ □$_{0.67}$(SiO$_4$)$_2$O$_2$; C: Er$_2$Si$_2$O$_7$, type *D*; D: Ho$_2$Si$_2$O$_7$, type *D*; E: Y$_2$Si$_2$O$_7$, type *D*.

Table 5. Atomic coordinates and displacement parameters for $EuVO_4$.

Atom	Site	x/a	y/b	z/c	U_{11}	U_{22}	U_{33}	U_{13}
Eu	4a	0	3/4	1/8	67(1)	67(1)	51(2)	0
V	4b	0	3/4	5/8	70(3)	70(3)	56(5)	0
O	16h	0	0.4315(4)	0.2036(5)	83(9)	181(11)	90(10)	12(8)

The U-values are multiplied by 10^4.

Table 6. Interatomic distances (in Å) in the zircon structure of $EuVO_4$, YVO_4 and $ErVO_4$.

$EuVO_4$		YVO_4 (Ref. 14)		$ErVO_4$ (Ref. 15)	
Eu–O	2.363(3)	Y–O	2.299±8	Er–O	2.27±2
Eu–O	2.474(3)	Y–O	2.443±8	Er–O	2.44±2
V–O	1.710(3)	V–O	1.706±8	V–O	1.72±2

space group $P2_1/c$. X-Ray diffraction data were measured as reported for $EuVO_4$, and cell parameters are listed in Table 3. Structure solution and refinement was also made as reported for $EuVO_4$. The final R-values were $R_F = 5.4\%$ and $R_w = 7.1\%$. Table 7 is a list of atomic coordinates and displacement parameters, and interatomic distances and bond lengths are in Table 8. Figure 1 is a stereoscopic drawing of the structure of $Ho_2Si_2O_7$, type D. A Fourier map calculation showed that the bridge oxygen atom O3 showed a rather large displacement perpendicular to the Si–O–Si bond direction shaped as a disc with its center 0.13 Å off the atomic position of O3. If the oxygen atom is placed in the centre, the Si–O–Si angle would be 172° in contrast to the value of 180° reported previously.[4]

Table 7. Structure parameters for $Ho_2Si_2O_7$, type D from X-ray single-crystal diffraction data. Monoclinic space group $P2_1/c$. Occupancy of O3 is 0.5. The equivalent isotropic thermal parameters are listed.

Atom	Site	x/a	y/b	z/c	U_{eq}[a]
Ho	4e	0.88855(3)	0.84940(2)	0.09314(3)	0.0049(3)
Si	4e	0.6389(2)	0.1114(1)	0.3566(2)	0.0044(9)
O1	4e	0.7923(7)	0.0517(3)	0.1346(6)	0.010(3)
O2	4e	0.8752(7)	0.1823(3)	0.5390(6)	0.008(3)
O3	4e	0.5064(31)	−0.0075(13)	0.4866(24)	0.013(2)
O4	4e	0.3793(7)	0.2016(3)	0.2491(6)	0.009(3)

$^a U_{eq} = (1/3)\ \Sigma_i\ \Sigma_j\ U_{ij} a_i^* a_j^* a_i a_j$.

Table 8. Interatomic distances (in Å) in the structure of $Ho_2Si_2O_7$, type D.

Ho–O4	2.245(4)	Si–O1	1.632(4)
Ho–O2	2.257(4)	Si–O2	1.619(4)
Ho–O1	2.260(4)	Si–O4	1.627(3)
Ho–O4	2.272(4)	Si–O3	1.622(4)
Ho–O2	2.288(4)	Si–O3	1.636(4)
Ho–O1	2.325(4)		

Neutron powder diffraction investigations of the rare-earth silicates.

Structure investigation of the apatites $RE_{9.33}\square_{0.67}(SiO_4)_6O_2$. The crystal structures of the rare-earth oxyapatites $RE_{9.33}\square_{0.67}(SiO_4)_6O_2$ were reported for Gd by Smolin and Shepelev[16] and for Ce and Dy by Belokoneva et al.,[17] respectively. These investigations were made with X-ray single-crystal diffraction data. The structures have two independent RE atoms, one in site 6h and one in site 4f with three 1/3 RE atoms statistically distributed in the fourfold site. Model calculations were made with neutron powder diffraction data of $La_{9.33}\square_{0.67}(SiO_4)_6O_2$ and $Nd_{9.33}\square_{0.67}(SiO_4)_6O_2$ using the published atomic coordinates[17] as starting parameters, and the least-squares profile refinement program FullProf.[18] The final parameters for the two structures are listed in Table 9. Interatomic distances for the REO_x coordintion polyhedra and for the SiO_4^{4-} ion are in Table 10, and Fig. 2 is a projection of the structure of $Nd_{9.33}\square_{0.67}(SiO_4)_6O_2$ along [001]. The La1 and Nd1 atoms are seven-coordinated with six oxygen atoms from

Table 9. Structure parameters for $La_{9.33}\square_{0.67}(SiO_4)_2O_2$ and $Nd_{9.33}\square_{0.67}(SiO_4)_6O_2$ from neutron powder diffraction data. Hexagonal space group $P6_3/m$.

Atom	Site	x/a	y/b	z/c	$B/Å^2$
$La_{9.33}\square_{0.67}(SiO_4)_2O_2{}^a$					
La1	6h	0.9844(5)	0.2274(4)	1/4	0.7(1)
La2	4f	1/3	2/3	0.0058(8)	0.8(1)
Si	6h	0.3719(7)	0.4050(6)	1/4	0.2(1)
O1	6h	0.4830(7)	0.3209(6)	1/4	1.8(1)
O2	6h	0.4684(6)	0.5947(6)	1/4	1.3(1)
O3	12i	0.2571(5)	0.3472(5)	0.0683(4)	2.0(1)
O4	2a	0	0	1/4	3.5(2)
$Nd_{9.33}\square_{0.67}(SiO_4)_2O_2{}^b$					
Nd1	6h	0.9881(4)	0.2306(3)	1/4	0.4(1)
Nd2	4f	1/3	2/3	0.0013(6)	0.9(1)
Si	6h	0.3697(5)	0.3998(6)	1/4	0.6(1)
O1	6h	0.4842(4)	0.3186(4)	1/4	1.4(1)
O2	6h	0.4722(4)	0.5969(4)	1/4	1.4(1)
O3	12i	0.2513(4)	0.3421(3)	0.0680(3)	1.7(1)
O4	2a	0	0	1/4	1.6(1)

Profile parameters and R-values from the program FullProf. $^a U = 0.202(5)$, $V = -0.586(5)$, $W = 0.550(7)$. Asymmetry parameters: 0.26(3), 0.09(1), 0.14(4). $R_P = 7.4\%$, $R_{WP} = 9.9\%$, $R_F = 9.2\%$. $^b U = 0.202$, $V = -0.557(4)$, $W = 0.517(6)$. Asymmetry parameters: 0.43(2), 0.07(1), −0.20(3). $R_P = 4.9\%$, $R_{WP} = 5.8\%$, $R_F = 6.5\%$.

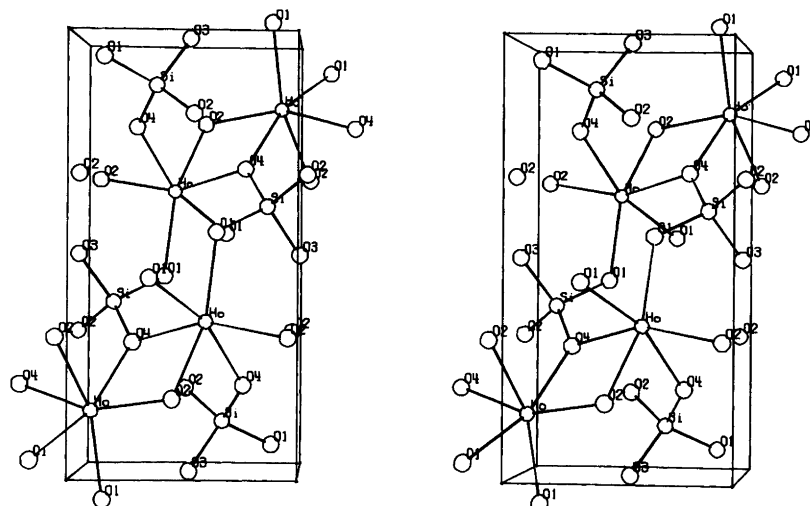*Fig. 1.* View of the structure of $Ho_2Si_2O_7$, type *D* along [100]. The *b*-axis is along the page.

Table 10. Interatomic distances in the structures of $La_{9.33}\square_{0.67}(SiO_4)_6O_2$ and in $Nd_{9.33}\square_{0.67}(SiO_4)_6O_2$.

La1–O4	2.29	La2–O2	2.49	Si–O2	1.60
La1–O3	2.46	La2–O2	2.49	Si–O3	1.63
La1–O3	2.46	La2–O2	2.49	Si–O3	1.63
La1–O2	2.56	La2–O1	2.52	Si–O1	1.65
La1–O3	2.65	La2–O1	2.52		
La1–O3	2.65	La2–O1	2.52		
La1–O1	2.71	La2–O3	2.85		
		La2–O3	2.85		
		La2–O3	2.85		
Nd1–O4	2.27	Nd2–O1	2.44	Si–O3	1.61
Nd1–O3	2.40	Nd2–O1	2.44	Si–O3	1.61
Nd1–O3	2.40	Nd2–O1	2.44	Si–O1	1.63
Nd1–O2	2.47	Nd2–O2	2.48	Si–O2	1.64
Nd1–O3	2.54	Nd2–O2	2.48		
Nd1–O2	2.54	Nd2–O2	2.48		
Nd1–O1	2.68	Nd2–O3	2.84		
		Nd2–O3	2.84		
		Nd2–O3	2.84		

the silicate ions, and with the free oxygen atom O4. The coordination polyhedron is a deformed version of the YO_7 coordination polyhedron found in the structure of YOOD.[19] The La2 and Nd2 atoms are nine-coordinated with oxygen atoms from the silicate ions. The coordination polyhedron is slightly deformed and of the same type as found in the structure of $Y(OH)_3$.[20] The La–O and Nd–O interatomic distances are within the expected range of distances, which is also the case for the Si–O distances of the SiO_4^{4-} ions in the two structures. The standard deviations found for the interatomic distances in the two structures are smaller than the errors reported in Ref. 16.

Structure investigation of $RE_2Si_2O_7$, Type D. Starting parameters for the model calculations using the neutron diffraction powder patterns of $Er_2Si_2O_7$, $Ho_2Si_2O_7$ and $Y_2Si_2O_7$ and the profile refinement program FullProf[18] were the parameters arrived at in the single-crystal structure analysis of $Ho_2Si_2O_7$ (see above). The final para-
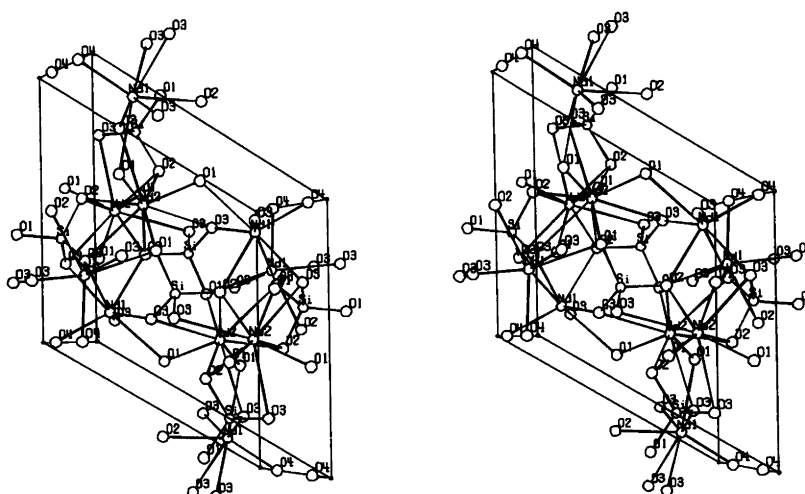

Fig. 2. View of the structure of $Nd_{9.33}\square_{0.67}(SiO_6)_4O_2$ along [001]. The *a*-axis is along the page.

Table 11. Structure parameters for $RE_2Si_2O_7$, type *D* from neutron powder diffraction data. Monoclinic space group $P2_1/c$; occupancy for O3 is 0.5.

Atom	Site	x/a	y/b	z/c	B/Å²
$Er_2Si_2O_7$[a]					
Er	4e	0.8913(12)	0.8495(4)	0.0941(10)	0.0(1)
Si	4e	0.6436(28)	0.1154(9)	0.3676(22)	1.3(2)
O1	4e	0.7885(14)	0.0493(6)	0.1354(13)	0.4(2)
O2	4e	0.8676(14)	0.1830(6)	0.5373(11)	0.0(1)
O3	4e	0.5285(37)	−0.0148(16)	0.4857(32)	0.0(2)
O4	4e	0.3802(16)	0.2031(6)	0.2501(14)	0.9(2)
$Y_2Si_2O_7$[b]					
Y	4e	0.8904(11)	0.8495(4)	0.0941(9)	0.4(1)
Si	4e	0.6445(2)	0.1136(8)	0.3696(17)	1.1(2)
O1	4e	0.7933(13)	0.0502(6)	0.1358(11)	0.6(1)
O2	4e	0.8670(12)	0.1822(5)	0.5371(10)	0.0(1)
O3	4e	0.5340(32)	−0.0106(16)	0.4976(32)	0.0(2)
O4	4e	0.3792(16)	0.2017(6)	0.2513(14)	2.0(2)
$Ho_2Si_2O_7$[c]					
Ho	4e	0.8950(13)	0.8492(4)	0.0964(11)	0.0(1)
Si	4e	0.6506(29)	0.1157(11)	0.3826(27)	1.8(3)
O1	4e	0.7922(18)	0.0487(8)	0.1374(15)	0.8(2)
O2	4e	0.8645(15)	0.1841(6)	0.5358(12)	0.0(2)
O3	4e	0.5445(32)	−0.0095(19)	0.5059(33)	0.0(3)
O4	4e	0.3826(23)	0.2021(9)	0.2549(21)	2.6(3)

Profile parameters and *R*-values from the program FullProf. [a]$U = 0.198$, $V = −0.554(5)$, $W = 0.553(9)$. Asymmetry parameters: $0.24(6)$, $0.03(2)$, $−0.02(7)$. $R_P = 6.8\%$, $R_{WP} = 8.9\%$, $R_F = 14.0\%$. [b]$U = 0.198(4)$, $V = −0.539(5)$, $W = 0.537(8)$. Asymmetry parameters: $0.31(5)$, $0.01(1)$, $−0.21(7)$. $R_P = 11.5\%$, $R_{WP} = 14.6\%$, $R_F = 12.5\%$. [c]$U = 0.206(5)$, $V = −0.559(5)$, $W = 0.554(11)$. Asymmetry parameters: $0.36(5)$, $0.04(2)$, $−0.13(7)$. $R_P = 6.8\%$, $R_{WP} = 9.1\%$, $R_F = 16.0\%$.

Table 12. Interatomic distances in the type *D* structures of $Ho_2Si_2O_7$, $Er_2Si_2O_7$ and $Y_2Si_2O_7$.

$Ho_2Si_2O_7$		$Er_2Si_2O_7$		$Y_2Si_2O_7$	
Ho–O1	2.24	Er–O1	2.23	Y–O1	2.24
Ho–O2	2.27	Er–O4	2.26	Y–O4	2.26
Ho–O4	2.27	Er–O4	2.26	Y–O4	2.27
Ho–O2	2.28	Er–O2	2.26	Y–O2	2.27
Ho–O4	2.31	Er–O2	2.29	Y–O2	2.30
Ho–O1	2.34	Er–O1	2.34	Y–O1	2.33
Si–O2	1.45	Si–O2	1.52	Si–O2	1.52
Si–O3	1.62	Si–O3	1.63	Si–O3	1.62
Si–O4	1.67	Si–O4	1.64	Si–O4	1.65
Si–O1	1.74	Si–O1	1.68	Si–O1	1.69

meters for the structures of the three compounds are listed in Table 11, and interatomic distances and bond angles are listed in Table 12.

In the RE_2SiO_7 type *D* structure the RE atoms are six-coordinated to oxygen atoms in a slightly deformed octahedron. In the disilicate ions the $Si–O_{bridge}$ distances are not significantly longer than the $Si–O_{terminal}$ distances. With the O_{bridge} atom placed statistically in site 4e the Si–O–Si angles cluster around the value 172°.

References

1. Christensen, A. N. *Z. Kristallogr. 209* (1994) 7.
2. Felsche, J. *J. Less-Common Met. 21* (1970) 1.
3. Dias, H. W., Glasser, F. P., Gunawardane, R. P. and Howie, R. A. *Z. Kristallogr. 191* (1990) 117.
4. Smolin, Yu. I. and Shepelev, Yu. F. *Acta Crystallogr., Sect. B26* (1970) 484.
5. Maqsood, A., Wanklyn, B. M. and Garton, G. *J. Cryst. Growth 46* (1979) 671.
6. Christensen, A. N. and Hazell, R. G. *Acta Chem. Scand. 45* (1991) 226.
7. Christensen, A. N. *Acta Chem. Scand. 46* (1992) 909.
8. Montorsi, M. *J. Less-Common Met. 84* (1982) 25.
9. Sheldrick, G. *SHELX86, Program for the Solution of Crystal Structures.* University of Göttingen, Germany 1986.
10. Busing, W. R., Martin, K. O. and Levy, H. A. *ORFLS, A Fortran Crystallographic Least Squares Program,* Report ORNL-TM 305. Oak Ridge National Laboratory, Oak Ridge, TN, 1962. LINUS is a 1971 version of ORFLS.
11. Cromer, D. T. and Waber, J. T. Report LA-3056, Los Alamos Scientific Laboratory of the University of California, Los Alamos, NM 1964.
12. Eds. MacGillavry, C.H., Rieck, G.D. and Lonsdale, K. *International Tables for X-Ray Crystallography,* The Kynoch Press, Birmingham, UK 1962, Vol. III, p. 213.
13. Schwarz, H. *Z. Anorg. Chem. 323* (1963) 44.
14. Baglio, J. A. and Gashurov, G. *Acta Crystallogr., Sect. B24* (1968) 292.
15. Patscheke, E., Fuess, H. and Will, G. *Chem. Phys. Lett. 2* (1968) 47.
16. Smolin, Yu. I. and Shepelev, Yu. F. *Izv. Akad. Nauk SSSR Neorg. Mat. 5* (1969) 1823.
17. Belokoneva, E. L., Petrova, T. L., Simonov, M. A. and Belov, N. V. *Sov. Phys. Crystallogr. 17* (1972) 429.
18. Rodriguez-Carvajal, J. *FullProf* Version 3.0.0. Apr. 95-LLBJRC. Laboratoire Léon Brillouin (CEA-CNRS), Saclay, France.
19. Christensen, A. N. and von Heidenstam, O. *Acta Chem. Scand. 20* (1966) 2658.
20. Christensen, A. N., Hazell, R. G. and Nilsson, Å. *Acta Chem. Scand. 21* (1967) 481.